Bandgap-Opened Bilayer Graphene Approached by Asymmetrical Intercalation of Trilayer Graphene

Da Zhan, Jia Xu Yan, Zhen Hua Ni, Li Sun, Lin Fei Lai, Lei Liu, Xiang Yang Liu, and Ze Xiang Shen**

Graphene is a kind of novel two dimensional material and considered as a potential candidate for nanoelectronics owing to its exotic electronic properties,[1] such as Massless Dirac Fermions, room-temperature quantum Hall effect,[2,3] Berry phase and Klein tunneling.[4,5] However, lacking a bandgap greatly limits the application of graphene in logic device, and hence the modification of graphene structures for opening its bandgap is indeed a crucial step towards the practical applications in logic-device-based nanoelectronics. To date, many methods have been theoretically predicted to open bandgap in graphene,[6–12] but only a few of them are experimentally proved, such as tailoring graphene atomic structure to form nanoribbons,[13] and adding an electrical gate voltage perpendicular to AB-stacked bilayer graphene (BLG) to break the inversion symmetry of the two equivalent layers.[14–17] For the former method, fabricating graphene nanoribbon needs a complicated procedure which would introduce defects unavoidably, as a consequence, its charge mobility significantly decreased;[18] For the latter method, in order to open a bandgap of ~0.2 eV, an extremely high effective electric field such as ~3 V/nm is required to break the inversion symmetry between top and bottom layers, which cannot be easily obtained except using specific polymer or ionic-liquid as the gated layer.[16,19] Recently, $FeCl_3$-based few-layer graphene intercalation has been experimentally achieved and this new structure has some exotic physical properties.[20–24] Khrapach et al. suggested that the $FeCl_3$-based intercalation of few-layer graphene with both high conductivity and transparency is comparable to indium tin oxide for solar cell applications,[22] and Bointon et al. reported that the magnetic ordering was discovered in this structure.[24] Furthermore, the intercalation induced strong doping can also engineer graphene's electronic band structure. Yang et al. theoretically demonstrated that an noticeable bandgap can be opened effectively if $FeCl_3$ is adsorbed on the surface of AB-stacked BLG.[25] We also notice that such modeled adsorption of $FeCl_3$ on graphene surface is unstable in ambient air and hence it cannot be used for practical applications.[21,26] Furthermore, the recently reported intercalation of $FeCl_3$ into the interspace of few-layer graphene not only induces strong charge doping for graphene to enhance its electrical conductivity, but also the new hybrid structure is very stable in ambient air because the outer graphene layers protect $FeCl_3$ from being deliquesced.[20] In this work, we started from using pristine trilayer graphene (**Figure 1**a) to prepare a novel graphene-based structure. In this new structure, one interlayer space of the trilayer graphene (TLG) is intercalated by $FeCl_3$ (Figure 1b) to form an asymmetrically intercalated trilayer graphene (AITG) structure along the z-direction. The charge transferring from the BLG to $FeCl_3$ breaks the electrostatic balance in the local space to form a quasi-electric-field that is perpendicular to the basal plane of BLG. It breaks the inversion symmetry between the top and bottom layers of BLG, and consequently, a prominent bandgap is expected to present in the separated BLG.[16,27] Furthermore, this novel graphene-based structure is proved to be very stable as both sides of $FeCl_3$ layer are protected by graphene. Therefore, realizing the ambient air stable and bandgap opened graphene-based configuration is a potential way towards future graphene-based application in nanoelectronics.

Raman spectroscopy has become a powerful tool to characterize graphene-based materials, including identifying number of layers, doping, defects, stacking, strain and edges,[20,23,28–39] in particular, the thickness and stacking sequence along z-direction can also be identified accurately.[20,21,28,40,41] The optical image of a pristine graphene

Dr. D. Zhan, Prof. X. Y. Liu
Research Institute for Soft Matter and Biomimetics
College of Materials & Department of Physics
Xiamen University
Xiamen 361005, China
E-mail: zhanda@xmu.edu.cn

Dr. D. Zhan, Dr. J. X. Yan, L. Sun,
Dr. L. F. Lai, Prof. Z. X. Shen
Centre for Disruptive Photonic Technologies
& Division of Physics and Applied Physics
School of Physical and Mathematical Sciences
Nanyang Technological University
637371, Singapore
E-mail: zexiang@ntu.edu.sg

Prof. Z. H. Ni
Department of Physics
Southeast University
Nanjing 211189, China

Prof. L. Liu
Key Laboratory of Luminescence
and Applications
CIOMP
Chinese Academy of Sciences, No.3888 Dongnanhu Road
Changchun 130033, China

DOI: 10.1002/smll.201402728

www.MaterialsViews.com

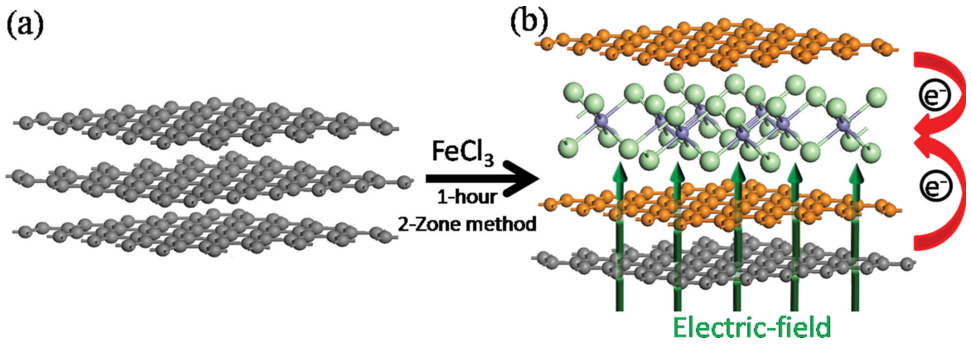

Figure 1. The schematic crystal structure evolution from pristine AB-stacked trilayer graphene (a) to the $FeCl_3$ asymmetrically intercalated trilayer graphene (out-of-plane) (b). The charge transfer effect forms a quasi-electric-field perpendicular to the BLG.

sample is shown in **Figure 2**a, which is uniform across the whole sample. Raman spectrum (Black curve in Figure 2c) and optical contrast spectra (Figure S1) indicate that this sample is TLG.[28,40] According to its Raman feature of 2D peak, we can also conclude that the TLG sample is in form of ABA stacking.[42–44] After the TLG physically reacted with $FeCl_3$ using the aforementioned modified recipe, it still presents very uniform optical contrast as shown in Figure 2b. But meanwhile, it is noticed that two regions present different Raman features and the corresponding Raman spectra are shown in Figure 2c. For the region *A*, the Raman *G* band consists of only one single Lorentzian peak, and the peak position blueshifts to ~1584 cm^{-1} indicating that it is lightly doped TLG as compared to pristine graphene of which the *G* band position normally located at ~1580 cm^{-1}. The slight blueshift of *G* band for region *A* should not be ascribed to the intercalation effect because of the very low doping level. It should be owing to surface molecular doping induced slight blueshift of *G* band. Such effect is normally observed for graphene samples that annealed in vacuum and then exposure to air.[27,30] For region *B*, the green curve of Raman spectrum presents two Lorentzian fitted *G* peaks respectively located at ~1590 (G^-) and ~1610 cm^{-1} (G^+) as shown in Figure 2c. For the previously reported full intercalated trilayer graphene, the blueshifted *G* bands at positions of ~1612 and ~1625 cm^{-1} are the signs for the graphene layers flanked on one and two sides by $FeCl_3$, respectively,[20,26] thus the region *B* should not be the full intercalated TLG due to absence of ~1625 cm^{-1} Raman peak. Furthermore, different from fully intercalated TLG in which the 2D band consists of only one single Lorentzian peak,[20] the 2D band of the structure modified TLG in region *B* consists of two obvious separated peaks with different intensity, located at ~2696 and ~2730 cm^{-1}, respectively. On the other hand, the Raman features for both G and 2D bands presented by region *B* are very similar to the nonhomogeneously doped BLG (With one graphene layer is heavily doped and the other layer is lightly doped) as shown by blue curve in Figure 2c.[27,29] Thus the crystal structure of region *B* is possibly the expected AITG structure as shown in Figure 1b, of which the new obtained crystal forms G-G-$FeCl_3$-G sequenced out-of-plane from bottom to up (The 'G' represents the graphene layer). Compared to the pristine ABA-stacked TLG shown

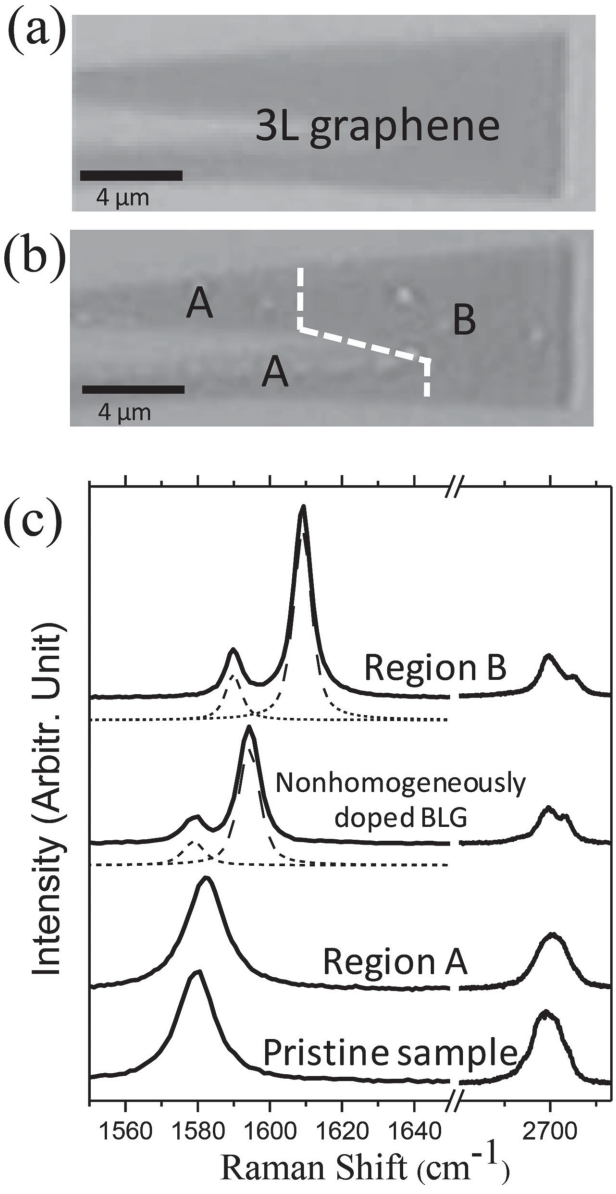

Figure 2. The optical images of the trilayer graphene sample before (a) and after (b) intercalation process. (c) Raman spectra for the pristine trilayer graphene, region A, region B, and one nonhomogeneously doped BLG (with one layer heavily doped and another layer lightly doped).

in Figure 1a, the schematic crystal structure of $FeCl_3$-AITG shown in Figure 1b consists of two independent graphene systems that are separated by $FeCl_3$ layer, one is single layer graphene (SLG) locates at above of the $FeCl_3$ and the other is AB-stacked BLG locates at below of the $FeCl_3$ (Figure 1b). As $FeCl_3$ is more electron-negative compared to pristine graphene, thus both the two independent graphene systems, the SLG and AB-stacked BLG must be hole doped by $FeCl_3$. Next, we will focus on discussing the independent AB-stacked BLG. Because the distance between $FeCl_3$ layer and each graphene layer of BLG is different, apparently, the adjacent graphene layer (brown-color layer in Figure 1b) is hole doped heavier compared to the other layer (grey-color layer in Figure 1b) which is relatively far away from $FeCl_3$. Therefore, the inequivalent doping level for the two layers would give rise to the inversion symmetry breaking effect for the AB-stacked BLG. In this case, the transformation of its representative point group from D_{3d} to C_{3V} occurs. And it causes the activation of G^- band, because the silent anti-symmetric vibration mode E_u at Γ point for D_{3d} group belongs to degenerated E representation for C_{3v} group. It is worth noting that the G^+ band is always active as it arises from the symmetric vibration phonon mode E_g at the Γ point of Brillouin zone. The much stronger intensity of $I_G{}^+$ compared to that of $I_G{}^-$ is another evidence to show that symmetry inversion of the AB-stacked BLG is broken.[29] For the SLG above $FeCl_3$ (Figure 1b), it can be considered as an quasi-independent SLG suffered strong hole-doping effect.[20] It is worth noting that another important function of this graphene layer is to protect $FeCl_3$ from being deliquesced in ambient air.[21]

The Raman images (**Figure 3**a,b) demonstrate a clearly identification of regions *A* and *B*. The G_0 (G^-) band (the G_0 band denotes the E_{2g} vibration mode in non-intercalated TLG) of region *A* presents obvious higher intensity, but the G^+ band is absence in this region. Contrarily, region *B* shows very strong intensity of G^+ band, but very weak for G^- band. Meanwhile, none of the regions present G_2 band (G_2 band represents the *G* band position blueshifted to >1620 cm^{-1} because the graphene layer is flanked on both sides by $FeCl_3$) (Figure S2),[20] indicating that there is no full intercalation of $FeCl_3$ for both regions *A* and *B*. Therefore, based on the information of Raman images, we conclude that there is no intercalation for region *A*, while region *B* is AITG which is uniform across the whole region. The height profile of transition region from *A* to *B* can be clearly seen by AFM image as shown in Figure 3c, the thickness of region *B* is ~0.61 nm thicker than that of region *A*. From previous theoretical works, the distance between adjacent graphene layers is expanded from 0.34 to 0.94 nm (0.6 nm thicker) after insertion of one $FeCl_3$ layer.[45] Thus, the AFM image further confirms that region *B* is AITG but not full intercalation as the experimental data is in agreement with the value reported theoretically and experimentally.[46,47] We should point out here that the indistinguishable optical contrast between region *A* and *B* is actually reasonable. This because that the intercalated one layer of $FeCl_3$ in region *B* does not affect the optical contrast obviously in visible region, which is in agreement with the most recent published results.[22]

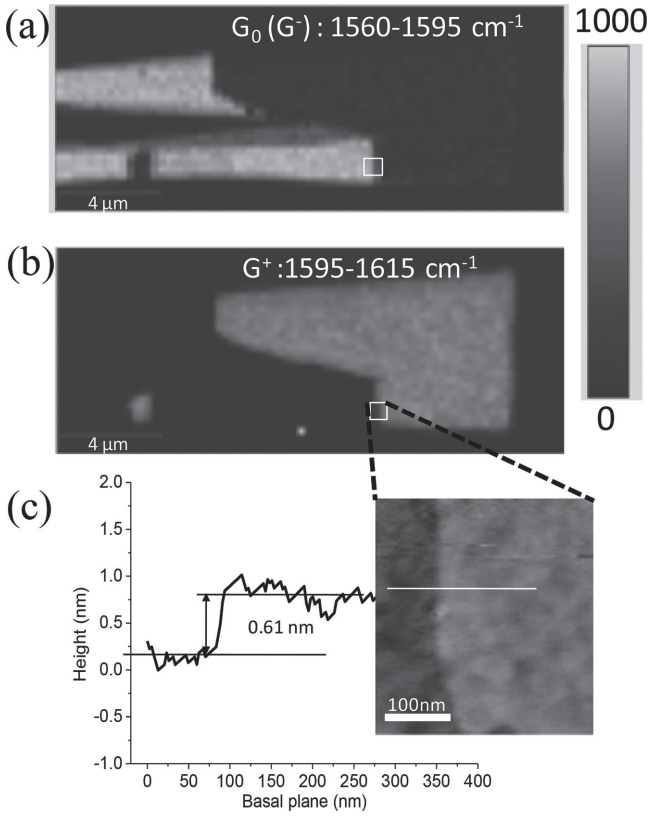

Figure 3. The Raman images for the trilayer graphene sample after $FeCl_3$ intercalation: (a) The G_0 band intensity with the integrated region from 1560 to 1595 cm^{-1}. (b) The G^+ band intensity with the integrated region from 1595 to 1615 cm^{-1}. (c) The AFM image of the white square region labeled in Raman images, and the cross section height profile of the white line is demonstrated as well.

For the AB-stacked BLG flanked by one side of $FeCl_3$, its inversion symmetry is broken due to the asymmetric doping level for the two electronic-coupled graphene layers, and hence it should present essential different electronic properties compared to that of pristine BLG, particularly that the bandgap may be opened.[27] To further examine the electronic structure difference between AITG and its precursor TLG with ABA stacking, we calculated their electronic band structures using First principles theory (the detailed calculation method is given at the experimental section at the end). As shown in **Figure 4**a, the electronic coupling effects between the adjacent layers give rise to the formation of four-fold degenerate zero-energy level for pristine TLG. The intercalated $FeCl_3$ in region *B* separates SLG and BLG leading to the band structures modified. As shown in Figure 4b, the electronic bands denoted by the red curves presenting linear dispersive behaviour arise from the separated SLG, and the Fermi level is downshifted ~0.58 eV with respect to the Dirac point. For the separated BLG below the $FeCl_3$ layer, it consists of two pairs of electronic bands: (π_1, $\pi_1{}^*$) and (π_2, $\pi_2{}^*$). For pristine BLG, the electronic bands π_1 and $\pi_1{}^*$ at low-energy regime touch each other at Dirac point,[48,49] but these two bands separated at Dirac point for BLG in AITG (Figure 4b). It is clearly seen that the separated electronic bands, π_1 and $\pi_1{}^*$, presenting an energy gap $\Delta E_k \approx 0.20$ eV at Dirac point, but it should be noticed that

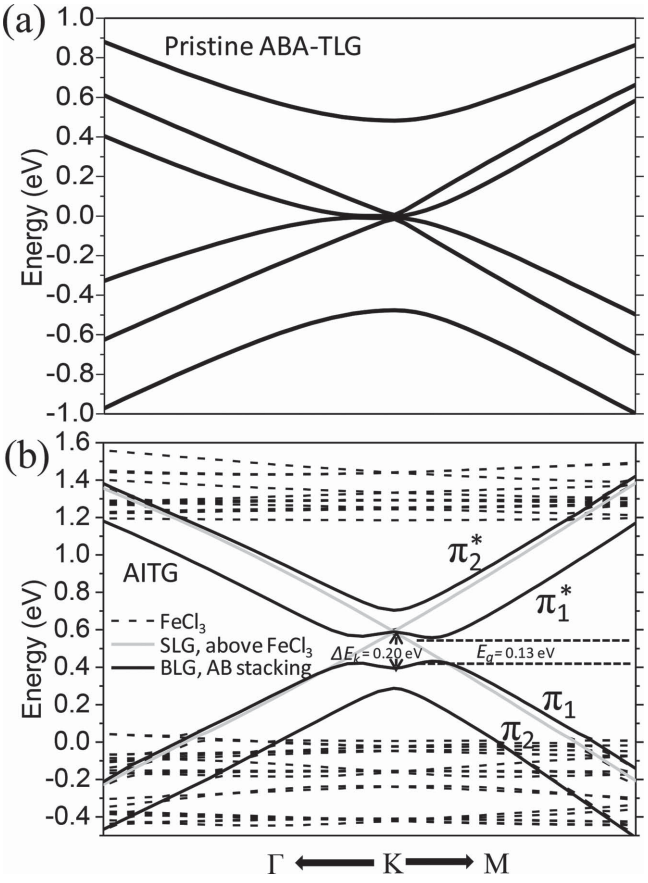

Figure 4. The electronic band structure around the Dirac point of the graphene sample: (a) The pristine trilayer graphene stacked in ABA geometry does not possess a bandgap. (b) The electronic bands of AITG can be divided into three independent parts: 1) the linear dispersive bands arise from the independent SLG (grey); 2) the bandgap opened BLG (black solid lines), the bandgap (E_g = 0.13 eV) and energy gap (ΔE_k = 0.20 eV) are clearly observed; 3) the $FeCl_3$ bands (black dashed lines).

the effective opened bandgap $E_g \approx 0.13$ eV is smaller than the energy gap ΔE_k as shown in Figure 4b. The theoretically calculated opened bandgap E_g and energy gap ΔE_k for inversion symmetry breaking BLG is in agreement with the recent calculated results.[25]

It is worth noting that to date, a lot of experimental works based on doping graphene chemically have been reported, but only a few dopants have been proved to achieve strong doping effect as high as 3×10^{13} cm^{-2},[20,21,25,50] and other dopants which adsorbed on graphene surface only present low-level doping due to the weak charge transfer effect, particularly for the commonly used organic compounds, such as triazine, An-CH_3, TCNQ, and TPA.[27,32,51] Notwithstanding the adsorption of triazine gives rise to relatively low-doping level for BLG, the bandgap of ~0.11 eV was still observed and the current on/off ratio was enhanced at least one-order compared to the pristine graphene sample.[27] Most recently, Park et al. experimentally fabricated the dual molecular (NH_2 and F4-TCNQ) doped BLG device,[52] and the opened bandgap was estimated to be larger than 0.16 eV although NH_2 and FE-TCNQ are not strong doping molecules. Therefore, the realization of such $FeCl_3$-AITG structure is also crucial for engineering graphene bandgap, particularly that the actual bandgap of the separated BLG should be even larger than the calculated result (~0.13 eV) as the bandgap value obtained by First principle method is normally smaller than the real case.[53] Electrical measurement of such $FeCl_3$-AITG structure should be carried out in the future to confirm the bandgap opening. Compared to other reported intercalants that can dope graphene strongly (such as Br_2 and I_2),[50] another advantage of using $FeCl_3$ for engineering the electronic band structure of few-layer graphene is its non-toxic.[22] Furthermore, the theoretically modeled BLG that adsorbed by $FeCl_3$ on surface is not stable in ambient air because $FeCl_3$ is a very active compound that can deliquesce easily by reacting with small amount of H_2O in ambient air,[21,25,26] but the experimentally fabricated $FeCl_3$-AITG structure shows very good environmental stability as we have not found any obvious changes since the sample was prepared four years ago. Furthermore, as shown in Figure S3, a very large TLG flake (~50 × 15 μm) with more than 2/3 area has been intercalated to form AITG structure by using the same preparation recipe as mentioned in this paper. Therefore, the preparation of AITG structure can be realized intentionally by controlling the reaction time. Here, we need to point out that based on our experience, the perfect controllability for fabricating AITG structure in a whole trilayer graphene flakes has not been achieved. To date, it is still a challenge because that the molecular dynamics for intercalation process is still unclear though it has been investigated for more than 40 years.[46] In addition to the reported asymmetrical intercalation of trilayer graphene in this paper, we can intuitively know that the asymmetrical intercalation of quad-layer graphene (AIQG) would probably present more interesting phenomenon. The AIQG structure has an order as G-G-G-$FeCl_3$-G along the z-direction (The 'G' represents the graphene layer). The G-G-G may have two forms which are ABA and ABC stacking, respectively. As each graphene layer in G-G-G is chemically doped in different level due to the different distance with respect to the $FeCl_3$ layer, the asymmetric doping effect on the G-G-G trilayer can be considered as a quasi-electric-field that is perpendicular to the basal plane of AIQG. In this case, the separated independent G-G-G trilayer would present the semimetal property if it is ABA stacking,[43,54,55] or else, it should present a relatively larger bandgap if it is ABC stacking.[43,55] Therefore, the proposed conception of the asymmetric intercalation of graphene induced interesting phenomenon is not only limited to trilayer case, but also available for quad-layer, and it is deserved for further studies in future.

In conclusion, the ambient air stable $FeCl_3$-based AITG structure has been prepared by using traditional two-zone method. The AITG's out-of-plane G-G-$FeCl_3$-G structure is confirmed by both Raman spectra and AFM images. Raman spectroscopy shows that compared to the pristine graphene, the *G* band of AITG split into two peaks with different intensity ($G^+ >> G^-$), which is similar to that of asymmetric doped BLG with a broken inversion symmetry; and the 0.6 nm height difference between non-intercalated TLG and AITG is in agreement with the previous theoretical prediction value. The giant blueshift of the high frequency G^+ peak indicates that the BLG in AITG is heavily doped, and the First

principle calculation shows that a 0.13 eV bandgap is opened for the separated BLG. The realization of bandgap opened and ambient air stable AITG structure opens a new route for graphene gap-engineering and it is essentially crucial for graphene-based nanoelectronic applications in the near future.

Experimental Section

AB-stacked TLG samples were deposited using conventional micromechanical cleavage method on silicon wafer coated by 300 nm SiO_2 layer. The layer number of graphene flakes were confirmed by both Raman[28,56] and contrast spectra.[40] It is reported by several groups including ours that $FeCl_3$-based full intercalated few-layer graphene can be fabricated using two-zone methods (with reaction time more than 6 hours).[20,21,26] To fabricate the aforementioned out-of-plane asymmetrical intercalated trilayer graphene (AITG), we controlled the reaction time for only ~1 hour, which is much shorter than the previously reported recipes,[20,21,26] and we will show the details of identification of such AITG by both Raman spectroscopy and AFM image later. Raman spectra were recorded by a Renishaw system with a spectral resolution of ~1 cm^{-1} (532 nm laser). Raman mappings were recorded by CRM200 system. A piezostage was used to move the substrate with a step size of 250 nm and Raman spectrum is recorded at every point in the scanned area. Density functional theory calculations were performed using Vienna *ab* initio Simulation Package (VASP).[57,58] Exchange correlation interactions were described by the generalized gradient approximation (GGA) in the Perdew-Burke-Ernzerhof (PBE) form.[59] For all systems, we used a kinetic cutoff energy of 400 eV. The Brillouin-zone integration was performed within Monkhorst-Pack scheme using a ($4 \times 4 \times 1$) mesh. All model structures are optimized with the vacuum separation set to be more than 10 Å.

Supporting Information

Supporting Information is available from the Wiley Online Library or from the author.

Acknowledgements

The work in Xiamen University was supported by NSFC (Grant No. 11404272) and the Fundamental Research Funds for the Central Universities (Grant No. 20720140514). The work in Southeast University was supported by NSFC (Grant No. 11104026, 61376104, and 61422503).

[1] A. A. Balandin, *Nat. Nanotechnol.* **2013**, *8*, 549–555.
[2] K. S. Novoselov, A. K. Geim, S. V. Morozov, D. Jiang, M. I. Katsnelson, I. V. Grigorieva, S. V. Dubonos, A. A. Firsov, *Nature* **2005**, *438*, 197–200.
[3] Y. B. Zhang, Y. W. Tan, H. L. Stormer, P. Kim, *Nature* **2005**, *438*, 201–204.
[4] M. I. Katsnelson, K. S. Novoselov, A. K. Geim, *Nat. Phys.* **2006**, *2*, 620–625.
[5] A. F. Young, P. Kim, *Nat. Phys.* **2009**, *5*, 222–226.
[6] Y. W. Son, M. L. Cohen, S. G. Louie, *Phys. Rev. Lett.* **2006**, *97*, 216803.
[7] L. Yang, C. H. Park, Y. W. Son, M. L. Cohen, S. G. Louie, *Phys. Rev. Lett.* **2007**, *99*, 186801.
[8] X. Y. Peng, R. Ahuja, *Nano Lett.* **2008**, *8*, 4464–4468.
[9] J. Berashevich, T. Chakraborty, *Phys. Rev. B* **2009**, *80*, 033404.
[10] P. Kim, *Nat. Mater.* **2010**, *9*, 792–793.
[11] D. C. Elias, R. R. Nair, T. M. G. Mohiuddin, S. V. Morozov, P. Blake, M. P. Halsall, A. C. Ferrari, D. W. Boukhvalov, M. I. Katsnelson, A. K. Geim, K. S. Novoselov, *Science* **2009**, *323*, 610–613.
[12] J. T. Wu, X. H. Shi, Y. J. Wei, *Acta Mechanica Sinica* **2012**, *28*, 1539–1544.
[13] M. Y. Han, B. Ozyilmaz, Y. B. Zhang, P. Kim, *Phys. Rev. Lett.* **2007**, *98*, 206805.
[14] T. Ohta, A. Bostwick, T. Seyller, K. Horn, E. Rotenberg, *Science* **2006**, *313*, 951–954.
[15] J. B. Oostinga, H. B. Heersche, X. L. Liu, A. F. Morpurgo, L. M. K. Vandersypen, *Nat. Mater.* **2008**, *7*, 151–157.
[16] Y. B. Zhang, T. T. Tang, C. Girit, Z. Hao, M. C. Martin, A. Zettl, M. F. Crommie, Y. R. Shen, F. Wang, *Nature* **2009**, *459*, 820–823.
[17] E. McCann, *Phys. Rev. B* **2006**, *74*, 161403.
[18] Z. H. Ni, L. A. Ponomarenko, R. R. Nair, R. Yang, S. Anissimova, I. V. Grigorieva, F. Schedin, P. Blake, Z. X. Shen, E. H. Hill, K. S. Novoselov, A. K. Geim, *Nano Lett.* **2010**, *10*, 3868–3872.
[19] J. T. Ye, M. F. Craciun, M. Koshino, S. Russo, S. Inoue, H. T. Yuan, H. Shimotani, A. F. Morpurgo, Y. Iwasa, *Proc. Natl. Acad. Sci. USA* **2011**, *108*, 13002–13006.
[20] D. Zhan, L. Sun, Z. H. Ni, L. Liu, X. F. Fan, Y. Y. Wang, T. Yu, Y. M. Lam, W. Huang, Z. X. Shen, *Adv. Funct. Mater.* **2010**, *20*, 3504–3509.
[21] W. J. Zhao, P. H. Tan, J. Liu, A. C. Ferrari, *J. Am. Chem. Soc.* **2011**, *133*, 5941–5946.
[22] I. Khrapach, F. Withers, T. H. Bointon, D. K. Polyushkin, W. L. Barnes, S. Russo, M. F. Craciun, *Adv. Mater.* **2012**, *24*, 2844–2849.
[23] X. Q. Zou, D. Zhan, X. F. Fan, D. Lee, S. K. Nair, L. Sun, Z. H. Ni, Z. Q. Luo, L. Liu, T. Yu, Z. X. Shen, E. E. M. Chia, *Appl. Phys. Lett.* **2010**, *97*, 141910.
[24] T. H. Bointon, I. Khrapach, R. Yakimova, A. V. Shytov, M. F. Craciun, S. Russo, *Nano Lett.* **2014**, *14*, 1751–1755.
[25] J. W. Yang, G. Lee, J. S. Kim, K. S. Kim, *J. Phys. Chem. Lett.* **2011**, *2*, 2577–2581.
[26] N. Kim, K. S. Kim, N. Jung, L. Brus, P. Kim, *Nano Lett.* **2011**, *11*, 860–865.
[27] W. Zhang, C.-T. Lin, K.-K. Liu, T. Tite, C.-Y. Su, C.-H. Chang, Y.-H. Lee, C.-W. Chu, K.-H. Wei, J.-L. Kuo, L.-J. Li, *ACS Nano* **2011**, *5*, 7517–7524.
[28] A. C. Ferrari, J. C. Meyer, V. Scardaci, C. Casiraghi, M. Lazzeri, F. Mauri, S. Piscanec, D. Jiang, K. S. Novoselov, S. Roth, A. K. Geim, *Phys. Rev. Lett.* **2006**, *97*, 187401.
[29] L. M. Malard, D. C. Elias, E. S. Alves, M. A. Pimenta, *Phys. Rev. Lett.* **2008**, *101*, 257401.
[30] Z. H. Ni, H. M. Wang, Z. Q. Luo, Y. Y. Wang, T. Yu, Y. H. Wu, Z. X. Shen, *J. Raman Spectrosc.* **2010**, *41*, 479–483.
[31] A. Das, S. Pisana, B. Chakraborty, S. Piscanec, S. K. Saha, U. V. Waghmare, K. S. Novoselov, H. R. Krishnamurthy, A. K. Geim, A. C. Ferrari, A. K. Sood, *Nat. Nanotechnol.* **2008**, *3*, 210–215.
[32] X. C. Dong, Y. M. Shi, Y. Zhao, D. M. Chen, J. Ye, Y. G. Yao, F. Gao, Z. H. Ni, T. Yu, Z. X. Shen, Y. X. Huang, P. Chen, L. J. Li, *Phys. Rev. Lett.* **2009**, *102*, 135501.
[33] A. Das, B. Chakraborty, A. K. Sood, *Bull. Mater. Sci.* **2008**, *31*, 579–584.
[34] Z. H. Ni, T. Yu, Y. H. Lu, Y. Y. Wang, Y. P. Feng, Z. X. Shen, *ACS Nano* **2008**, *2*, 2301–2305.

[35] S. Mathew, T. K. Chan, D. Zhan, K. Gopinadhan, A. R. Barman, M. B. H. Breese, S. Dhar, Z. X. Shen, T. Venkatesan, J. T. L. Thong, *Carbon* **2011**, *49*, 1720–1726.
[36] Y. M. You, Z. H. Ni, T. Yu, Z. X. Shen, *Appl. Phys. Lett.* **2008**, *93*, 163112.
[37] A. K. Gupta, T. J. Russin, H. R. Gutierrez, P. C. Eklund, *ACS Nano* **2009**, *3*, 45–52.
[38] Y. N. Xu, D. Zhan, L. Liu, H. Suo, Z. H. Ni, T. T. Nguyen, C. Zhao, Z. X. Shen, *ACS Nano* **2011**, *5*, 147–152.
[39] D. Zhan, L. Liu, Y. N. Xu, Z. H. Ni, J. X. Yan, C. Zhao, Z. X. Shen, *Sci. Rep.* **2011**, *1*, 12.
[40] Z. H. Ni, H. M. Wang, J. Kasim, H. M. Fan, T. Yu, Y. H. Wu, Y. P. Feng, Z. X. Shen, *Nano Lett.* **2007**, *7*, 2758–2763.
[41] D. F. Li, D. Zhan, J. X. Yan, C. L. Sun, Z. W. Li, Z. H. Ni, L. Liu, Z. X. Shen, *J. Raman Spectrosc.* **2013**, *44*, 86–91.
[42] C. H. Lui, Z. Q. Li, Z. Y. Chen, P. V. Klimov, L. E. Brus, T. F. Heinz, *Nano Lett.* **2011**, *11*, 164–169.
[43] S. H. Jhang, M. F. Craciun, S. Schmidmeier, S. Tokumitsu, S. Russo, M. Yamamoto, Y. Skourski, J. Wosnitza, S. Tarucha, J. Eroms, C. Strunk, *Phys. Rev. B* **2011**, *84*, 161408.
[44] C. X. Cong, T. Yu, K. Sato, J. Z. Shang, R. Saito, G. F. Dresselhaus, M. S. Dresselhaus, *ACS Nano* **2011**, *5*, 8760–8768.
[45] N. Caswell, S. A. Solin, *Solid State Commun.* **1978**, *27*, 961–967.
[46] M. S. Dresselhaus, G. Dresselhaus, *Adv. Phys.* **2002**, *51*, 1–186.
[47] C. Underhill, S. Y. Leung, G. Dresselhaus, M. S. Dresselhaus, *Solid State Commun.* **1979**, *29*, 769–774.
[48] E. McCann, V. I. Fal'ko, *Phys. Rev. Lett.* **2006**, *96*, 086805.
[49] E. McCann, D. S. L. Abergel, V. I. Fal'ko, *Solid State Commun.* **2007**, *143*, 110–115.
[50] N. Jung, N. Kim, S. Jockusch, N. J. Turro, P. Kim, L. Brus, *Nano Lett.* **2009**, *9*, 4133–4137.
[51] X. C. Dong, D. L. Fu, W. J. Fang, Y. M. Shi, P. Chen, L. J. Li, *Small* **2009**, *5*, 1422–1426.
[52] J. Park, S. B. Jo, Y. J. Yu, Y. Kim, W. Yang, W. H. Lee, H. H. Kim, B. H. Hong, P. Kim, K. Cho, K. S. Kim, *Adv. Mater.* **2012**, *24*, 407–411.
[53] M. S. Hybertsen, S. G. Louie, *Phys. Rev. B* **1986**, *34*, 5390–5413.
[54] M. F. Craciun, S. Russo, M. Yamamoto, J. B. Oostinga, A. F. Morpurgo, S. Tarucha, *Nat. Nanotechnol.* **2009**, *4*, 383–388.
[55] C. H. Lui, Z. Q. Li, K. F. Mak, E. Cappelluti, T. F. Heinz, *Nat. Phys.* **2011**, *7*, 944–947.
[56] Y. Y. Wang, Z. H. Ni, Z. X. Shen, H. M. Wang, Y. H. Wu, *Appl. Phys. Lett.* **2008**, *92*, 043121.
[57] K. Hoshino, F. Shimojo, *J. Phys. Condens. Matter.* **1996**, *8*, 9315–9319.
[58] G. Kresse, J. Furthmuller, *Comput. Mater. Sci.* **1996**, *6*, 15–50.
[59] J. P. Perdew, K. Burke, M. Ernzerhof, *Phys. Rev. Lett.* **1996**, *77*, 3865–3868.

Received: September 10, 2014
Revised: September 22, 2014
Published online: December 2, 2014